

Received February 3, 2021, accepted February 14, 2021, date of publication February 16, 2021, date of current version February 25, 2021.

Digital Object Identifier 10.1109/ACCESS.2021.3059948

# A Stacked Patch Antenna With Broadband Circular Polarization and Flat Gains

KANG DING<sup>1</sup>, YANJIE WU<sup>1</sup>, KUN-HUA WEN<sup>1</sup>, DUO-LONG WU<sup>1,2</sup>, (Member, IEEE),  
AND JIAN-FENG LI<sup>1,2</sup>

<sup>1</sup>School of Physics and Optoelectronic Engineering, Guangdong University of Technology, Guangzhou 510006, China

<sup>2</sup>State Key Laboratory of Precision Electronic Manufacturing Technology and Equipment, School of Electromechanical Engineering, Guangdong University of Technology, Guangzhou 510006, China

Corresponding author: Yanjie Wu (wuyanjie@gdut.edu.cn)

This work was supported in part by the Natural Science Foundation of Guangdong Province under Grant 2020A1515010442, in part by the National Natural Science Foundation of China under Grant U2001601 and Grant 61901126, and in part by the Science and Technology Project of Guangzhou under Grant 201904010243.

**ABSTRACT** In this paper, a stacked circular polarization (CP) patch antenna with broad impedance bandwidth, axial-ratio (AR) bandwidth, and flat gains is investigated. The antenna is composed of a square ring, double layers' stacked patches, and four vertical patches. The corner truncated loop served as a sequential phase feeding structure for four driven patches. To improve the impedance matching, four square patches are stacked on the bottom layer. Furthermore, four vertical patches are introduced on the ground plane to broaden the AR bandwidth. Simulated and measured studies are conducted on an antenna prototype to validate the proposed design. The proposed design shows that the measured impedance bandwidth is 4.65–7.21 GHz (43.2%), measured 3-dB AR bandwidth at broadside is 4.9–6.4 GHz (26.5%) and the 1-dB gain bandwidth is 4.75–6.6 GHz (32.6%). Compared with other similar CP stacked patch antennas, the antenna owns advantages of wide bandwidth, compact size, and flat gain.

**INDEX TERMS** Broadband antenna, circular polarization, stacked antenna, patch antenna.

## I. INTRODUCTION

Due to the advantages of suppressing multipath interferences and reducing polarization mismatch, some wireless communication systems require the antenna to have wideband and CP characteristics [1], [2]. Besides, CP antennas with wide bandwidth, compact size, and flat gain are necessary to meet the demand for high data rate transmission and processing [3]–[6].

To achieve the broadband operation, many antennas have been proposed accordingly, such as dipole antennas [7]–[9], dielectric resonator antennas [10], and microstrip patch antennas. Crossed dipoles [11], [12] or cross-bowtie antenna [13] are commonly used structures for achieving wideband CP operation due to their orthogonal feed method. In [11], parasitic loops were introduced to a printed crossed dipole to generate one extra CP mode. Moreover, the CP bandwidth can be enhanced to 106.1% by using metallic plates [12]. However, metallic reflectors [11], [12] or artificial magnetic conductor (AMC) reflector [13] are usually

required in the design, and therefore, cavity-backed ground planes with a high profile and complex structure are needed. Among the CP antenna designs, single-fed patch antennas are much preferred owing to their compact structure. However, single-fed microstrip patch antennas always have narrow AR bandwidth [14]. Consequently, many investigations have been conducted to enhance their AR bandwidth [15]–[17]. A widely used method for achieving broadband CP operation is to use stacked patches [18]–[20]. Rotated stacked rectangular patches were presented in [21] to achieve a 3-dB AR bandwidth of 33.6%. However, the wide AR bandwidths were obtained at the expense of large size and high profile. In [22], a perturbed ring resonator with a pin-loaded structure was proposed to realize a wider AR bandwidth as well as high gain. However, the narrow AR bandwidth (6%) is not enough for wideband systems. In addition, the sequential phase feed technique was developed in [23] to increase the AR bandwidth with a stacked structure. An E-shaped patch was also employed in [24] and near-field resonant parasitic (NFRP) patch was used to further improve the bandwidth. Besides, parasitic elements were also employed to increase bandwidth in [25]. A substrate integrated suspended line antenna was

The associate editor coordinating the review of this manuscript and approving it for publication was Raghvendra Kumar Chaudhary.

proposed in [26] to achieve broadband impedance matching and wideband CP characteristics. Another kind of stacked antenna with wideband CP operation is metasurface-based stacked antenna [27]–[30]. Although excellent performance is obtained, periodic cells are usually needed leading to an increase of the design complexity.

To obtain wide 3-dB AR bandwidth and flat gain, a stacked patch antenna with coupled vertical patches is developed in this paper. The square loop is initially proposed to obtain the original CP mode, then the double layers' stacked structure is employed not only to improve the impedance matching but also to generate extra CP mode. Moreover, four vertical walls are embedded on the ground plane to enhance CP performance. A fabricated antenna model is used to verify the simulation results.

II. ANTENNA DESIGN

A. ANTENNA CONFIGURATION

The geometry of the proposed broadband CP stacked antenna is shown in Fig. 1. The proposed structure is composed of a coaxial-fed square loop, double layers' stacked patches, and vertical patches embedded on the ground plane. The square ring fabricated on the bottom substrate ( $\epsilon_r = 2.2$ ,  $\tan \delta = 0.001$ ) works as a feeding network, so a minimum AR point can be obtained by exciting the fundamental one-wavelength mode of the loop [4]. On the basis of the origin loop, a double layers' stacked structure is introduced. The stacked patches are printed on the top layer of substrate ( $\epsilon_r = 2.2$ ,  $\tan \delta = 0.001$ ), and the gap between the top and bottom layer is  $h_3$ . The impedance matching is improved by introducing the double layers' stacked structure, and extra CP mode is also generated at the upper band. Meanwhile, the gain at the upper band is also improved, and therefore wide gain bandwidth is also enhanced by the stacked patches. In order to improve CP performance, four vertical patches are sequentially placed on the ground plane. The designed structure is simulated by ANSYS HFSS to obtain both wide impedance bandwidth and CP bandwidth. The optimized parameters of the design are shown in Table 1.

TABLE 1. Parameter of the stacked antenna (unit: mm).

symbol	value	symbol	value
$l_1$	12.9	$l_2$	9
$r_1$	1	$r_2$	3
$d$	4.5	$d_1$	0.65
$d_2$	6.5	$g$	0.4
$c$	1.5	$w_d$	12
$w_s$	12	$l$	18
$h$	6	$h_1$	1
$h_2$	2	$h_3$	2
$W_1$	44	$W_2$	38

B. EVOLUTION PROCESSES

To clarify the design procedure, five different prototypes in Fig. 2 are studied. Ant.1 is a traditional microstrip square

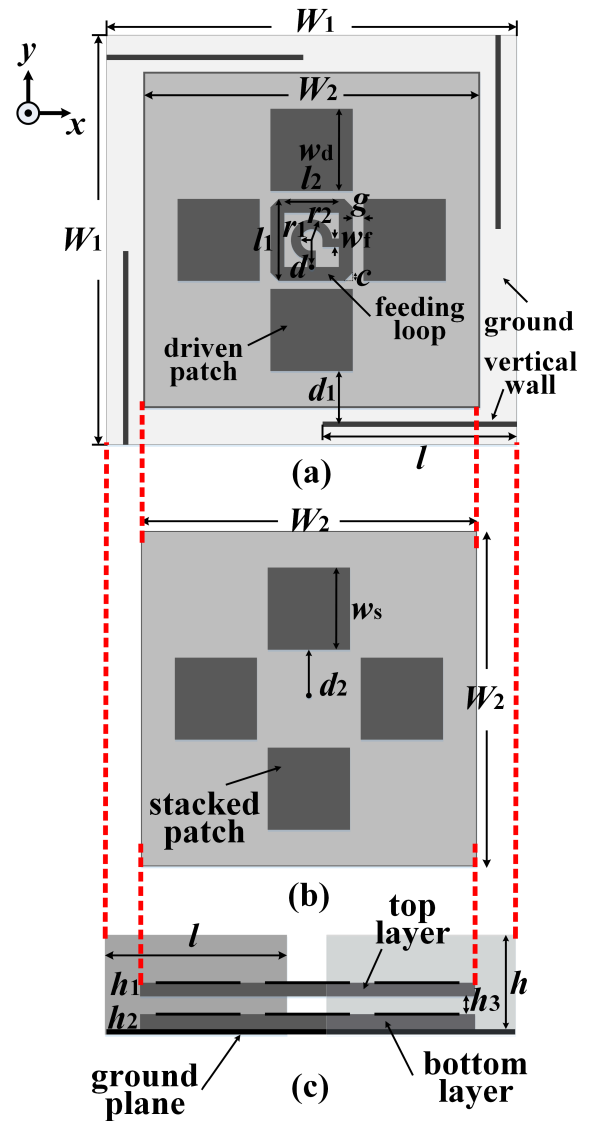


FIGURE 1. Configurations of the proposed antenna. (a) bottom layer. (b) top layer. (c) side view.

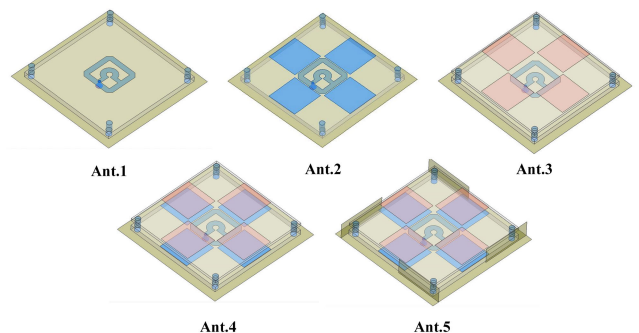
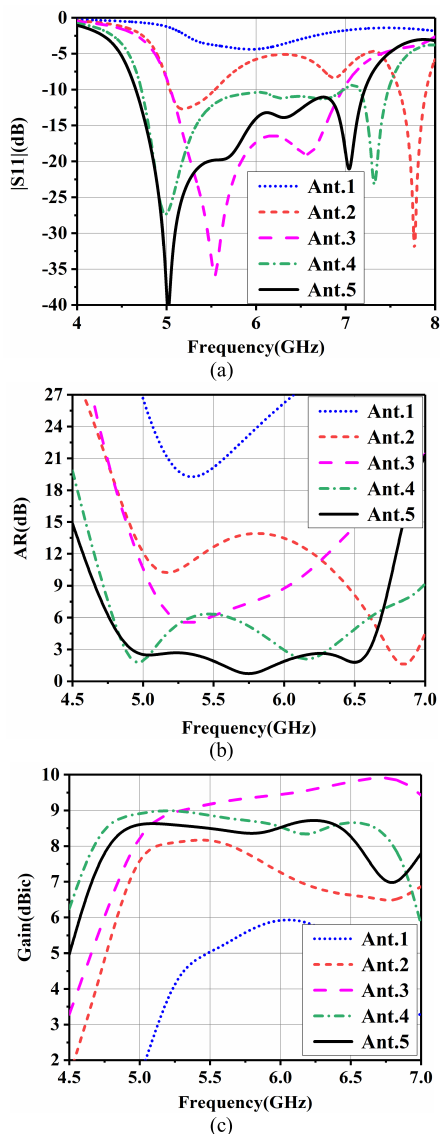


FIGURE 2. Various stages of evolution of the designed antenna.

ring antenna with arc-shaped delay line. The arc-shaped delay line inside of the square-ring radiator has a length of  $\lambda_g/4$ , so 90° phase difference for CP operation is achieved. Ant.2 is



**FIGURE 3.** Simulated results of the designed antenna at different stages: (a) S-parameter, (b) AR, (c) Gain.

a loop antenna with surrounding driven patches. In Ant.3, four stacked patches are introduced to Ant.1. Ant.4 combined the surrounding driven patches and stacked patches together. Four vertical patches are applied in Ant.4 to form Ant.5. In order to provide a comprehensive comparison, simulated results of An.1 to Ant.5 are shown in Fig. 3. In general, the square ring antenna possesses a narrow impedance bandwidth due to the large input impedance. Hence, Ant. 1 owns only one resonance at 6.0 GHz and the impedance matching is poor, as shown in Fig. 3(a). To increase the impedance bandwidth, Ant.2 is loaded with four driven patches which are placed around the loop antenna. By the capacitive coupling between the loop and the driven patches, another two resonances and a new AR minimum point at 6.7 GHz are yielded due to the sequential phase provided by the loop antenna. However, the resonances are far from each other, and cannot

be combined together to obtain wide bandwidth. Besides, the gains at the upper band decrease dramatically, and thus the 3-dB gain bandwidth is also narrow. In order to improve the antenna performance, only four stacked patches are introduced to Ant.1. For Ant.3, both the impedance matching and gain bandwidth are enhanced. The improved impedance bandwidth is due to the coupling between the stacked patch layer and driven patch layer. Besides, the stacked patch are arranged in a loop way to obtain loose coupling. And the two resonant frequencies at 5.5 and 6.6 GHz of Ant.3 is attributed to the driven patch and stacked patch respectively. Meanwhile, the AR value of Ant. 3 is also reduced when it is compared with Ant.1. However, it can be seen from the curve that Ant.3 cannot obtain wide CP bandwidth since it has only one minimum AR point. By combining the surrounding patches and stacked patches simultaneously, wide 10-dB impedance bandwidth from 4.75 GHz to 7.5 GHz is obtained for Ant.4.

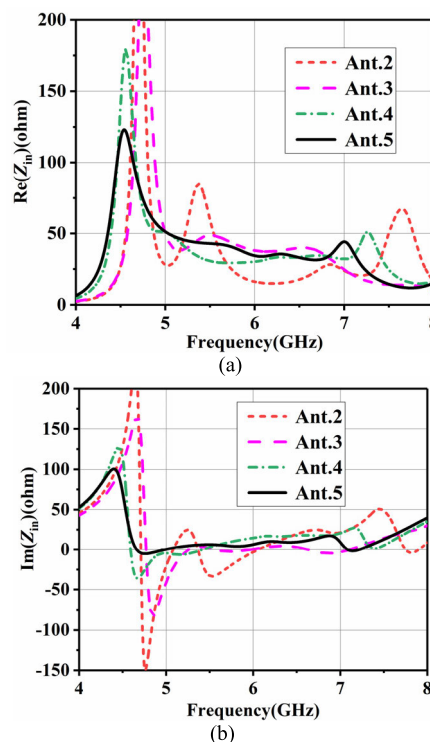


**FIGURE 4.** Input impedance of different antennas: (a) real part, (b) imaginary part.

Fig. 4 shows the simulated input impedance of different antennas. With the help of stacked patches, the real part of input impedance is closer to  $50 \Omega$  and the imaginary part also fluctuates around  $0 \Omega$ . The results shows the impedance matching is greatly improved. Furthermore, the gains at the upper band also increase and flat gain in the whole band is realized by introducing the stacked patches. However, the ARs are still high than 3 dB from 5.2 to 6.0 GHz which is because the two AR minimum are far away. To extend the CP bandwidth, four vertical patches are embedded on the

four corners of the ground plane. Finally, Ant.4 is evaluated into Ant.5. Actually, the vertical patches could be regarded as modified conducting walls which have proven to be a good way to increase bandwidth in [8] and [31]. The studied results in [8], [31] indicated that the radiation of cavity-based antenna consists of two parts, including original radiation and surrounding walls. When the primary radiator is excited, the walls are energized by the radiation coupling, and then the radiation aperture formed by the walls act as additional radiator. It has been pointed out in [8] and [31] that the additional radiator can improve the antenna's performances, which produce wider impedance and AR bandwidth when compared with those traditional reflector without vertical walls. In this design, the modified walls are introduced to generate a new AR minimum point at 5.75 GHz is introduced, leading to an extended CP bandwidth of 29.9% (4.90–6.62 GHz). It is worth mentioning that the AR bandwidth of Ant.4 is not the optimal result since the dimensions are directly copied from the optimized wideband design that has vertical patches. Furthermore, the impedance matching is also improved by the vertical patches.

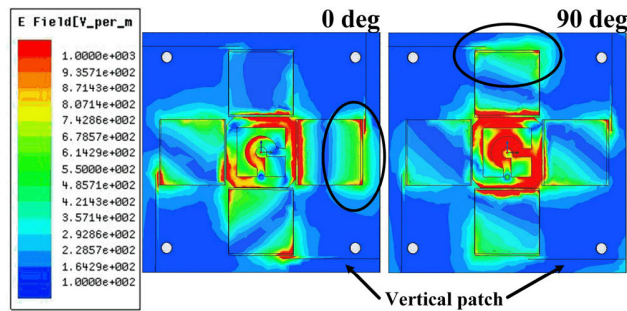


FIGURE 5. Simulated E-field distribution of the proposed antenna at 5.75 GHz.

The electric field distribution at 5.75 GHz is investigated in Fig. 5, and different distributions of E-field with different phases are observed. Furthermore, it can be seen that the currents concentrate on the feeding loop and surrounding coupled patches. At  $0^\circ$  phase, the maximum E-field focuses on the right part and strong field distribution is observed between the stacked patches and vertical patches. When it comes to the  $90^\circ$  phase, a strong E-field occurs at the top part. Comparing with the field distribution results, it can be deduced that vertical patches contribute to the generation of CP mode. To explain the working principle of this CP antenna, vector current distributions on the upper layer and lower layer were investigated. They are illustrated in Fig. 6 over a period corresponding to the frequency of 5.75 GHz. At the phase of  $0^\circ$ , the dominant current flows in the vertical direction, whereas at the phase of  $90^\circ$  the dominant currents flow in the horizontal direction. Besides, it is clear that a right-hand CP (RHCP) wave toward the  $+z$ -direction is generated.

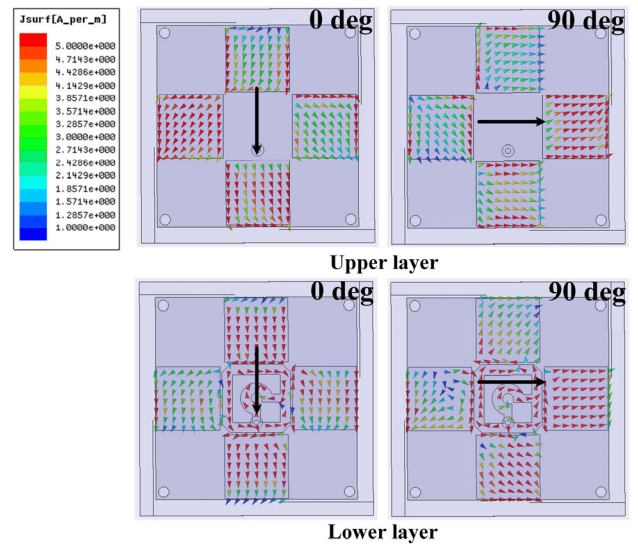


FIGURE 6. Vector current distributions of the stacked CP antenna at 5.75 GHz.

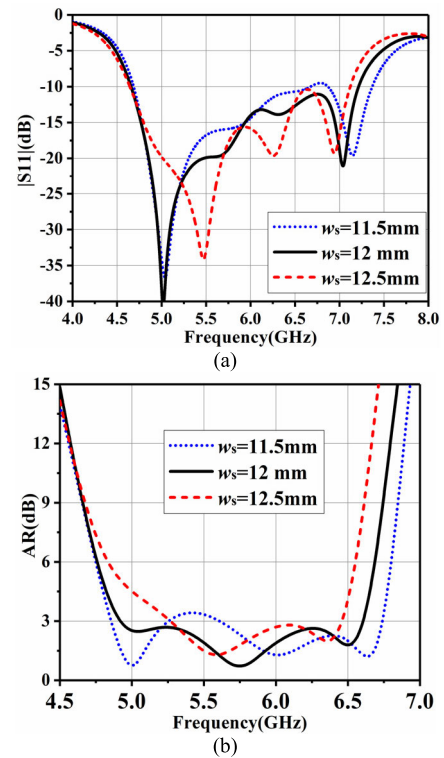
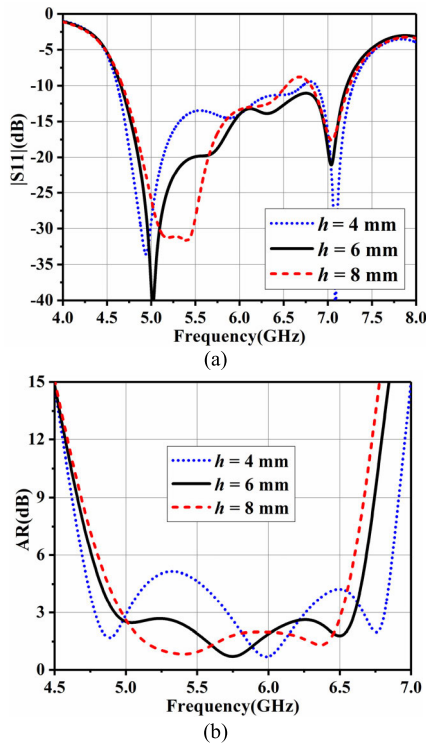


FIGURE 7. Effect of  $w_s$  on the performance of the proposed antenna: (a) S-parameter, (b) AR.

C. PARAMETRIC STUDIES

To verify the operating mechanism of the proposed stacked wideband CP patch antenna, a parametric analysis is discussed in this section. Fig. 7 shows the simulated  $|S_{11}|$  and ARs with different  $w_s$  which is defined as the length of the stacked patch. From the figure, it could be observed





**FIGURE 8.** Effect of  $h$  on the performance of the proposed antenna: (a) S-parameter, (b) AR.

that the  $|S_{11}|$  has slight shifts at the upper band while it is greatly affected at the lower band with different  $w_s$ . A wide impedance bandwidth is achieved when  $w_s$  is selected as 12 mm. As  $w_s$  increases from 11.5 to 12.5 mm by a step size of 0.5 mm, the CP mode at the upper band shifts downward and the ARs at 5.0 GHz get worse. The results indicate that the CP performance at the higher band is affected by the stacked patches and  $w_s$  could be used as an important parameter to tune the value of AR at the lower band.

Fig. 8 depicts the simulated results under the different height of the vertical patch. As for  $|S_{11}|$ , obvious effect is seen at the lower band. With the decreases of  $h$ , the impedance matching at 5.5 GHz gets worse. In Fig. 8(b), the resonant frequency at the upper band shifts upward as  $h$  decrease from 8 to 4 mm. Meanwhile, the variation of  $h$  has a notable impact on the lower band ARs, which indicates the vertical patches contribute to the CP performance in the whole band. The influences of  $h_3$  are also studied in Fig. 9. The results indicate that the  $|S_{11}|$  is not sensitive to the variation of  $h_3$ . Moreover, the gap between the two substrates only affects the CP property at the lower band. The  $h_3$  is changed from 1.5 to 2.5 mm, leading to great change at the lower frequency but little change at the upper frequency. Therefore, we could utilize the appropriate gap to optimize the ARs at the lower band.

Based on the parameter analysis, a design principle is summarized as follows:

1) First, design a loop antenna with four surrounding patches to cover the lower and upper band, respectively.

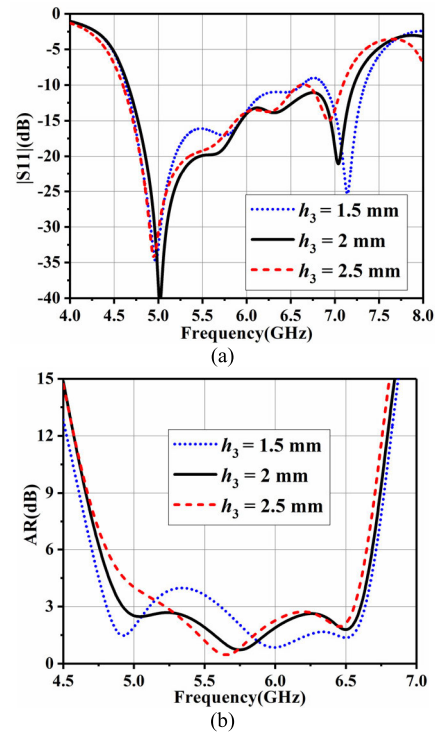


**FIGURE 9.** Effect of  $h_3$  on the performance of the proposed antenna: (a) S-parameter, (b) AR.

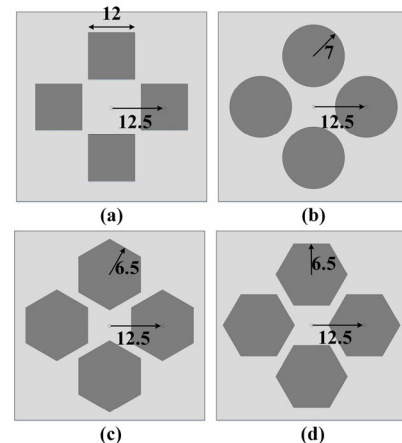


**FIGURE 10.** Stacked antennas with different shapes: (a) Square, (b) Circle, (c) Hexagon-1, (d) Hexagon-2.

2) Second, place four stacked patches above the bottom layer to improve the impedance matching.

3) Third, add four vertical patches around the antenna to improve the CP performance at upper band.

4) Lastly, tune each parameter to optimize the design for optimal bandwidth.

**D. COMPARISON OF DIFFERENT STACKED PATCHES**

Four different stacked patches are studied for comparison. The stacked patch examples are shown in Fig. 10, where all the dimensions are in millimeter. The distance between the patch element and the center of the substrate slab is

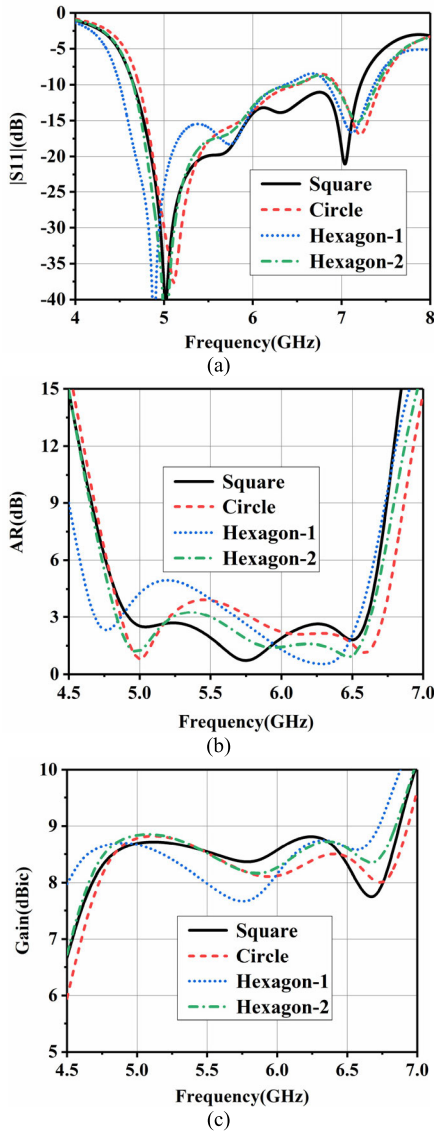


FIGURE 11. Simulated results of the designed antenna with different stacked patches: (a) S-parameter, (b) AR, (c) Gain.

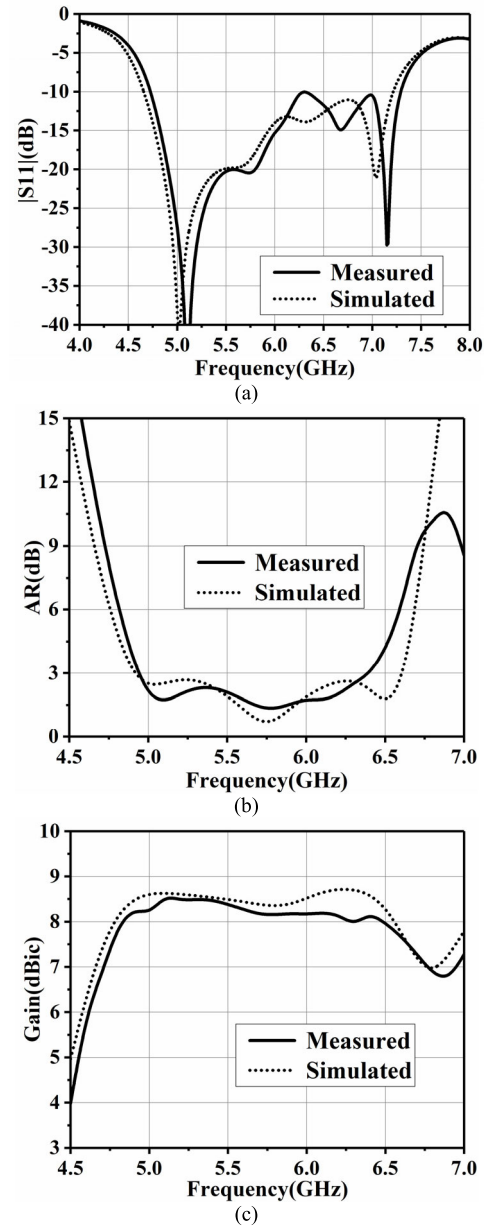


FIGURE 13. Simulated and measured results of the stacked antenna. (a)  $|S_{11}|$ . (b) AR. (c) Gain.

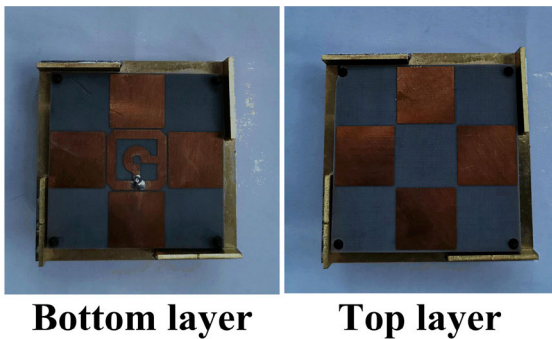


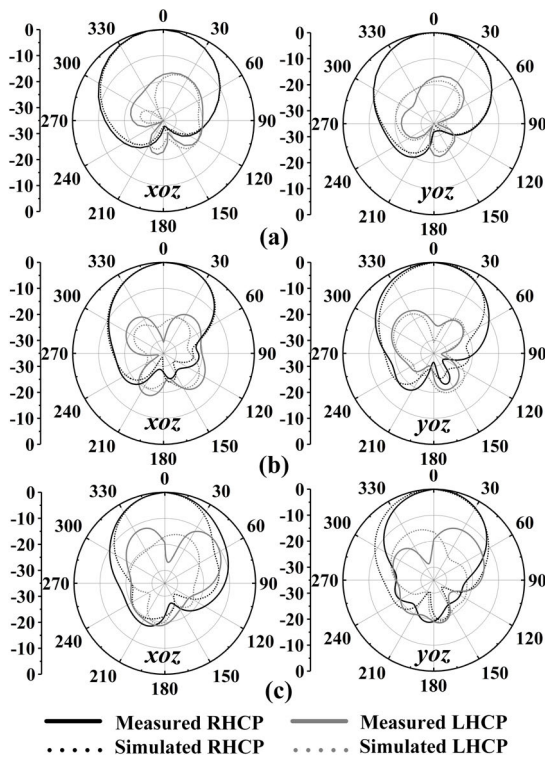
FIGURE 12. Photograph of the fabricated prototype.

fixed (12.5 mm) for all examples. The square-, circular, and two hexagonal stacked patches performances are compared in Fig. 11. The resonant frequency at upper band has small

shifts with different shapes of stacked patches. The square patch shows the lowest resonant frequency at upper band. It is noted that the impedance match at high frequencies is poor for circular and hexagonal patches as the resonant frequencies are far apart from the other resonance points. The same phenomenon also occurs for AR and gain curves. The ARs in middle band are affected due to the shifting of minimum AR points. In addition, greater influences for hexagon-1 patches is observed because the hexagon-1 shaped patches with sharp corners lead to the coupled surface current with vertical patches flowing in a unsmooth path. In this paper, the square patches are chosen as stacked patches to obtain a wider bandwidth. The reason that the square patches are selected is mainly because straight edges could bring about

**TABLE 2.** Comparison of different cp stacked patch antennas.

Ref	Volume ( $\lambda_0^3$ )	Impedance bandwidth	AR bandwidth	1-dB gain bandwidth	Peak gain(dBic)
[20]	$0.8 \times 0.8 \times 0.09$	31.5%	20.7%	16.7%	8.6
[23]	$1.5 \times 1.5 \times 0.058$	20.8 %	17.6%	9.7%	11.5
[26]	$2.4 \times 2.4 \times 0.102$	20.2 %	18.9%	10.8%	13.8
[28]	$1.0 \times 1.0 \times 0.068$	25.7%	8%	8.3%	8.0
<b>Our work</b>	<b><math>0.88 \times 0.88 \times 0.12</math></b>	<b>43.2%</b>	<b>26.5%</b>	<b>32.6%</b>	<b>8.5</b>

**FIGURE 14.** Measured and simulated radiation patterns in  $xoz$  and  $yoz$  planes at: (a) 5.0 GHz, (b) 5.75 GHz, (c) 6.2 GHz.

surface current flowing through smooth paths when they are coupled with the nearby vertical walls.

### III. EXPERIMENTAL VERIFICATION

To verify the performance of our stacked antenna, the designed antenna is fabricated and measured. The antenna prototype is shown in Fig. 12, which is composed of two substrates. The comparison of simulated and measured results is illustrated in Fig. 13. It can be seen that the designed antenna is able to obtain a good impedance matching from 4.65 to 7.21 GHz (43.2%), which is in good agreement with the simulated results. The measured AR results are also compared with simulated results in Fig. 13(b). The 3-dB AR bandwidth is from 4.9 to 6.4 GHz, or a fractional bandwidth of 26.5%. Fig. 13(c) illustrates the measured gain at the broadside direction and its CP gain of 8.5 dBic is obtained at 5.2 GHz. Besides, the measured 1-dB gain bandwidth is around 32.6% (4.75–6.6 GHz). Flat gain with a variation of less than 1 dB is realized within the operating frequency. Fig. 14 shows the normalized radiation pattern in the  $xoz$

and  $yoz$ -planes at different frequencies. It is observed that the RHCP level is 18 dB stronger than the LHCP components at the broadside direction, which indicates a good RHCP antenna. Table 2 summarized the performances of our designed stacked CP antenna, where  $\lambda_0$  is the wavelength at the center frequency of passband. The compared results with other similar stacked antennas in the literature is listed. It indicates that the designed stacked CP antenna has wider bandwidth including impedance, AR, and 1-dB gain bandwidth among the reported designs.

### IV. CONCLUSION

In this paper, a stacked patch antenna with wide bandwidth and flat gains has been proposed. Moreover, four vertical patches are embedded on the ground plane to broaden the CP bandwidth. An antenna prototype is fabricated and measured. The measurement results indicate that the designed antenna can exhibit an impedance bandwidth of 43.2%, and a CP bandwidth of 26.5%. Besides, a flat gain is also obtained within the operating frequency.

### REFERENCES

- [1] J. Wang, Y. Li, L. Ge, J. Wang, M. Chen, Z. Zhang, and Z. Li, "Millimeter-wave wideband circularly polarized planar complementary source antenna with endfire radiation," *IEEE Trans. Antennas Propag.*, vol. 66, no. 7, pp. 3317–3326, Jul. 2018.
- [2] B. Zhang, Y. P. Zhang, D. Titz, F. Ferrero, and C. Luxey, "A circularly-polarized array antenna using linearly-polarized sub grid arrays for highly-integrated 60-GHz radio," *IEEE Trans. Antennas Propag.*, vol. 61, no. 1, pp. 436–439, Jan. 2013.
- [3] G. Li and F.-S. Zhang, "A compact broadband and wide beam circularly polarized antenna with shorted vertical plates," *IEEE Access*, vol. 7, pp. 90916–90921, 2019.
- [4] C. Deng, Y. Li, Z. Zhang, and Z. Feng, "A wideband sequential-phase fed circularly polarized patch array," *IEEE Trans. Antennas Propag.*, vol. 62, no. 7, pp. 3890–3893, Jul. 2014.
- [5] Y. Li, Z. Zhang, and Z. Feng, "A sequential-phase feed using a circularly polarized shorted loop structure," *IEEE Trans. Antennas Propag.*, vol. 61, no. 3, pp. 1443–1447, Mar. 2013.
- [6] K. Ding, C. Gao, T. Yu, D. Qu, and B. Zhang, "Gain-improved broadband circularly polarized antenna array with parasitic patches," *IEEE Antennas Wireless Propag. Lett.*, vol. 16, pp. 1468–1471, 2017.
- [7] L. Wang, W.-X. Fang, W.-H. Shao, B. Yao, Y. Huang, and Y.-F. En, "Broadband circularly polarized cross-dipole antenna with multiple modes," *IEEE Access*, vol. 8, pp. 66489–66494, 2020.
- [8] T. K. Nguyen, H. H. Tran, and N. Nguyen-Trong, "A wideband dual-cavity-backed circularly polarized crossed dipole antenna," *IEEE Antennas Wireless Propag. Lett.*, vol. 16, pp. 3135–3138, 2017.
- [9] S. X. Ta, K. Lee, I. Park, and R. W. Ziolkowski, "Compact crossed-dipole antennas loaded with near-field resonant parasitic elements," *IEEE Trans. Antennas Propag.*, vol. 65, no. 2, pp. 482–488, Feb. 2017.
- [10] Y.-D. Zhou, Y.-C. Jiao, Z.-B. Weng, and T. Ni, "A novel single-fed wide dual-band circularly polarized dielectric resonator antenna," *IEEE Antennas Wireless Propag. Lett.*, vol. 15, pp. 930–933, 2016.



- [11] J.-W. Baik, T.-H. Lee, S. Pyo, S.-M. Han, J. Jeong, and Y.-S. Kim, "Broadband circularly polarized crossed dipole with parasitic loop resonators and its arrays," *IEEE Trans. Antennas Propag.*, vol. 59, no. 1, pp. 80–88, Jan. 2011.
- [12] Y. M. Pan, W. J. Yang, S. Y. Zheng, and P. F. Hu, "Design of wideband circularly polarized antenna using coupled rotated vertical metallic plates," *IEEE Trans. Antennas Propag.*, vol. 66, no. 1, pp. 42–49, Jan. 2018.
- [13] W. Lin, S. L. Chen, R. W. Ziolkowski, and Y. J. Guo, "Reconfigurable wideband low-profile circularly polarized antenna and array enabled by artificial magnetic conductor ground," *IEEE Trans. Antennas Propag.*, vol. 66, no. 3, pp. 1564–1569, Mar. 2018.
- [14] O. P. Falade, M. U. Rehman, Y. Gao, X. Chen, and C. G. Parini, "Single feed stacked patch circular polarized antenna for triple band GPS receivers," *IEEE Trans. Antennas Propag.*, vol. 60, no. 10, pp. 4479–4484, Oct. 2012.
- [15] J. Wu, Y. Yin, Z. Wang, and R. Lian, "Broadband circularly polarized patch antenna with parasitic strips," *IEEE Antennas Wireless Propag. Lett.*, vol. 14, pp. 559–562, 2015.
- [16] K. Ding, C. Gao, D. Qu, and Q. Yin, "Compact broadband circularly polarized antenna with parasitic patches," *IEEE Trans. Antennas Propag.*, vol. 65, no. 9, pp. 4854–4857, Sep. 2017.
- [17] W. Yang, W. Sun, W. Qin, J. Chen, and J. Zhou, "Broadband circularly polarised stacked patch antenna with integrated dual-feeding network," *IET Microw., Antennas Propag.*, vol. 11, no. 12, pp. 1791–1795, Sep. 2017.
- [18] X. Chen, G. Fu, S.-X. Gong, Y.-L. Yan, and W. Zhao, "Circularly polarized stacked annular-ring microstrip antenna with integrated feeding network for UHF RFID readers," *IEEE Antennas Wireless Propag. Lett.*, vol. 9, pp. 542–545, 2010.
- [19] S. Shekhawat, P. Sekra, D. Bhatnagar, V. K. Saxena, and J. S. Saini, "Stacked arrangement of rectangular microstrip patches for circularly polarized broadband performance," *IEEE Antennas Wireless Propag. Lett.*, vol. 9, pp. 910–913, 2010.
- [20] W. Yang, J. Zhou, Z. Yu, and L. Li, "Single-fed low profile broadband circularly polarized stacked patch antenna," *IEEE Trans. Antennas Propag.*, vol. 62, no. 10, pp. 5406–5410, Oct. 2014.
- [21] H. Oraizi and R. Pazoki, "Wideband circularly polarized aperture-fed rotated stacked patch antenna," *IEEE Trans. Antennas Propag.*, vol. 61, no. 3, pp. 1048–1054, Mar. 2013.
- [22] Z.-X. Liu, L. Zhu, and X. Zhang, "A low-profile and high-gain CP patch antenna with improved AR bandwidth via perturbed ring resonator," *IEEE Antennas Wireless Propag. Lett.*, vol. 18, no. 2, pp. 397–401, Feb. 2019.
- [23] W. Yang, J. Zhou, Z. Yu, and L. Li, "Bandwidth- and gain-enhanced circularly polarized antenna array using sequential phase feed," *IEEE Antennas Wireless Propag. Lett.*, vol. 13, pp. 1215–1218, 2014.
- [24] J. Li, H. Liu, S. Zhang, M. Luo, Y. Zhang, and S. He, "A wideband single-fed, circularly-polarized patch antenna with enhanced axial ratio bandwidth for UHF RFID reader applications," *IEEE Access*, vol. 6, pp. 55883–55892, 2018.
- [25] N. Hussain, H. H. Tran, and T. T. Le, "Single-layer wideband high-gain circularly polarized patch antenna with parasitic elements," *AEU-Int. J. Electron. Commun.*, vol. 113, Jan. 2020, Art. no. 152992.
- [26] N. Yan, K. Ma, and Y. Luo, "An SISL sequentially rotated feeding circularly polarized stacked patch antenna array," *IEEE Trans. Antennas Propag.*, vol. 68, no. 3, pp. 2060–2067, Mar. 2020.
- [27] N. Hussain, M.-J. Jeong, A. Abbas, T.-J. Kim, and N. Kim, "A metasurface-based low-profile wideband circularly polarized patch antenna for 5G millimeter-wave systems," *IEEE Access*, vol. 8, pp. 22127–22135, 2020.
- [28] H. L. Zhu, S. W. Cheung, K. L. Chung, and T. I. Yuk, "Linear-to-circular polarization conversion using metasurface," *IEEE Trans. Antennas Propag.*, vol. 61, no. 9, pp. 4615–4623, Sep. 2013.
- [29] N. Nasimuddin, Z. N. Chen, and X. Qing, "Bandwidth enhancement of a single-feed circularly polarized antenna using a metasurface: Metamaterial-based wideband CP rectangular microstrip antenna," *IEEE Antennas Propag. Mag.*, vol. 58, no. 2, pp. 39–46, Apr. 2016.
- [30] N. Hussain, M.-J. Jeong, A. Abbas, and N. Kim, "Metasurface-based single-layer wideband circularly polarized MIMO antenna for 5G millimeter-wave systems," *IEEE Access*, vol. 8, pp. 130293–130304, 2020.
- [31] L. Zhang, S. Gao, Q. Luo, P. R. Young, Q. Li, Y.-L. Geng, and R. A. Abd-Alhameed, "Single-feed ultra-wideband circularly polarized antenna with enhanced front-to-back ratio," *IEEE Trans. Antennas Propag.*, vol. 64, no. 1, pp. 355–360, Jan. 2016.



**KANG DING** was born in Jiangsu, China. He received the B.S. degree in communications engineering from the Nanjing University of Posts and Telecommunications, Nanjing, China, in 2011, and the M.S. and Ph.D. degrees from the PLA University of Science and Technology, Nanjing, in 2014 and 2017, respectively, both in electrical engineering. From 2015 to 2017, he was a Visiting Student with the Department of Electrical and Computer Engineering, National University of Singapore, Singapore. His research interests include antenna design and theory, particularly in broadband antennas and circularly polarized antenna design. He has served as a Reviewer for the *IEEE TRANSACTIONS ON ANTENNAS AND PROPAGATION*, the *IEEE ANTENNAS AND WIRELESS PROPAGATION LETTERS*, *IEEE ACCESS*, and the *IET Microwaves, Antennas and Propagation*.



**YANJIE WU** was born in Henan, China. He received the B.S. and M.S. degrees from Central South University, Changsha, China, in 2003 and 2006, respectively, and the Ph.D. degree from Sun Yat-sen University, Guangzhou, China, in 2015. From 2016 to 2017, he was a Visiting Scholar with the Department of Electrical and Computer Engineering, National University of Singapore, Singapore. He is currently working with the Guangdong University of Technology, Guangzhou. His current research interests include UWB antennas, MIMO antennas, base station antennas, and circularly polarized antennas.



**KUN-HUA WEN** received the B.E. and Ph.D. degrees from Southwest Jiaotong University, Chengdu, China, in 2007 and 2013, respectively. He is currently an Associate Professor with the Guangdong University of Technology, Guangzhou, China. He has authored and coauthored more than 50 articles published in distinguished peer-review journals. His current research interests include nano-photonics, optical sensing, and optical fiber Bragg grating.



**DUO-LONG WU** (Member, IEEE) was born in Tongcheng, Anhui, China. He received the B.S., M.S., and Ph.D. degrees from the University of Electronic Science and Technology of China, Chengdu, China, in 1987, 1995, and 1998, respectively. From 1998 to 2000, he was a Postdoctoral Fellow with Changhong Electric Company Ltd., Mianyang, China, and the University of Electronic Science and Technology of China. From 2002 to 2003, he was a Research Fellow with Nanyang Technological University, Singapore. From 2015 to 2016, he was a Visiting Scholar with Linköping University, Norrköping, Sweden. He is currently with the RF and 5G Communications Group, Guangdong University of Technology. His current research interests include RF, antennas, and wireless sensor networks.



**JIAN-FENG LI** was born in Maoming, Guangdong, China. She received the Ph.D. degree from the South China University of Technology, Guangzhou, Guangdong, in 2013. She is currently a Teacher with the Guangdong University of Technology, Guangzhou. Her research interests include phone antennas, multiband antennas, MIMO antennas, filtering antennas, UWB antennas, and base station antennas. She serves as a Reviewer for several journals, including the *IEEE*

*TRANSACTIONS ON ANTENNAS AND PROPAGATION*, the *IEEE TRANSACTIONS ON VEHICULAR TECHNOLOGY*, and *IEEE ANTENNAS AND WIRELESS PROPAGATION LETTERS*.

• • •